International Journal of Biological Macromolecules 277 (2024) 134113

Contents lists available at ScienceDirect

International Journal of Biological Macromolecules

journal homepage: www.elsevier.com/locate/ijbiomac

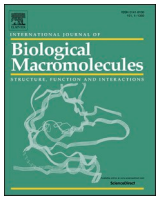

Interaction between antidepressant drug trazodone with double-stranded DNA: Multi-spectroscopic and computational analysis

Ambrish Kumar [a], Moumita Saha [a], Juhi Saraswat [b], Kamalakanta Behera [c,*], Shruti Trivedi [a,*]

[a] Centre of Advanced Studies, Department of Chemistry, Banaras Hindu University, Varanasi 221005, India
[b] Centre for Interdisciplinary Research in Basic Sciences, Jamia Millia Islamia, New Delhi 110025, India
[c] Department of Chemistry, University of Allahabad, Prayagraj 211002, India

ARTICLE INFO

Keywords:
Antidepressant
DNA
Drug-DNA interaction
Spectroscopy
Trazodone

ABSTRACT

Trazodone (TZD) is an antidepressant drug used to treat major depressive and sleeping disorders. Elevated doses of trazodone are associated with central nervous system depression, which manifests as nausea, drowsiness, confusion, vertigo, exhaustion, etc. To develop a clinically viable active pharmaceutical compound with minimal adverse effects, it is imperative to possess a comprehensive knowledge of the drug's action mechanism on DNA. Hence, we investigate the mode of interaction between trazodone and DNA utilizing various spectroscopic and computational techniques. Studies using UV–vis titration showed that the DNA and trazodone have an effective interaction. The magnitude of the Stern-Volmer constant (K_{SV}) has been calculated to be 5.84×10^6 M^{-1} by the Lehrer equation from a steady-state fluorescence study. UV–vis absorption, DNA melting, dye displacement, and circular dichroism studies suggested that trazodone binds with DNA in minor grooves. Molecular docking and molecular dynamic simulation demonstrated that the TZD-DNA system was stable, and the mode of binding was minor groove. Furthermore, ionic strength investigation demonstrates that DNA and trazodone do not have a substantial electrostatic binding interaction.

1. Introduction

Deoxyribonucleic acid (DNA) is necessary not only for the seamless operation of numerous body systems, but also for regulating vital processes including cell survival, transcription, and proliferation. Molecular growth and metabolism can be influenced by the topological and mechanical modifications of DNA induced by drugs. Organic compounds, both natural and synthetic, frequently approach DNA at the molecular scale [1]. The investigation of the interaction between small pharmaceutical compounds and DNA has sparked widespread scientific interest. This is not only for the advancement of DNA-targeted drug developments and effective tracking of the structure of nucleic acids but also because it provides crucial data for the evolution of therapeutic agents that regulate the expression of genes [2]. A variety of interactive forces interact in a complex manner to facilitate the identification of DNA bindings. It comprises intercalation between neighboring base pairs, binding with the minor and major grooves, and electrostatic interaction. The stability of the DNA-drug complex is attributed to several non-covalent interactions, including hydrogen bonds, van der Waals interactions, and hydrophobic forces [3].

Depression is a highly prevalent psychiatric disorder nowadays in society. Antidepressants are beneficial in the treatment of symptoms caused by depression [4]. Regretfully, these drugs are also given for numerous on-label and off-label diseases, including pain, migraine, eating disorders, quitting smoking, and deficit/hyperactivity disorders. This results in a spike in the consumption of antidepressant drugs, which may be intentional or unintentional, and gives rise to clinical and forensic instances of overdose [5]. Antidepressants constitute a category of substances that are often identified in forensic toxicology samples and are capable of inducing fatal intoxications [6]. Trazodone (TZD) is a psychoactive substance that belongs to the piperazine class and is available only by prescription. The Food and Drug Administration (FDA) has authorized its use to treat depression. Trazodone is a derivative of triazolopyridine which suppresses histamine and alpha-1-adrenergic receptors and inhibits serotonin reuptake. Trazodone is distinguished by its structural dissimilarity to other classes of antidepressants and its distinctive profile [7]. The chemical structure of trazodone hydrochloride is depicted in Fig. 1. Trazodone is usually well tolerated, and patients with co-occurring major depressive disorder and trouble sleeping may experience additional benefits [8]. Elevated doses of trazodone are

* Corresponding authors.
E-mail addresses: kamala.iitd@gmail.com (K. Behera), shrutitrivedi@bhu.ac.in (S. Trivedi).

https://doi.org/10.1016/j.ijbiomac.2024.134113
Received 11 May 2024; Received in revised form 17 July 2024; Accepted 21 July 2024
Available online 22 July 2024

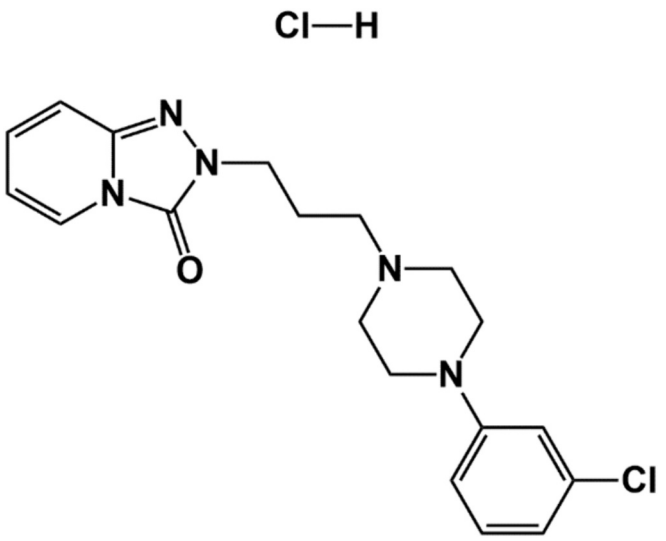

Fig. 1. The chemical structure of trazodone hydrochloride.

associated with central nervous system depression, hallucinations, delusions, impaired speech, seizures, respiratory arrest, and death [9]. To develop a clinically viable active pharmaceutical compound with minimal adverse effects, it is imperative to possess a comprehensive understanding of the cell and its unique characteristics, in addition to elucidating the underlying mechanism of action. Therefore, it is crucial to establish analytical techniques that can ascertain the nature of drug-DNA interactions, the specific principles governing these interactions, and the manner in which they occur [10].

A growing interest has emerged in the recent few years regarding the analysis of the interaction between DNA and drugs utilizing a variety of analytical approaches. Multiple interaction mechanisms between drugs and DNA have been identified, encompassing nucleoside-analog incorporation, covalent cross-linking/binding, groove binding, DNA cleavage, and drug-DNA intercalation [11]. It was believed that the majority of planar aromatic molecules bound to DNA primarily in an intercalative fashion, while crescent-shaped molecules favored groove binding. However, no specificity has been established depending on the structure-binding connection [12]. Therefore, the objective of this research is to give an understanding of trazodone and DNA interaction through the utilization of molecular multi-spectroscopic techniques, thereby contributing to the resolution of the existing knowledge gaps in pharmacokinetics.

2. Materials and methods

2.1. Materials

The sodium salt of DNA (Na-DNA) isolated from salmon testes was procured from Sigma-Aldrich Co. and stored in the refrigerator to maintain a low storage temperature (2–8 °C). Owing to its purity, it was used exactly as received, requiring no further processing. Trazodone hydrochloride (≥99 %, HPLC), Trizma® hydrochloride buffer solution (pH 7.4), ethidium bromide (≥95 % HPLC, BioReagent), rhodamine B (≥95 %, HPLC), sodium chloride (≥99 %, ACS reagent), were also purchase from Sigma-Aldrich Co. and utilized without any additional purification. HPLC-grade water was utilized throughout the experiment and purchased from Merck Life Science Pvt. Ltd. Conductivity of HPLC-grade water was measured by Eutech CON 700, ThermoFisher Scientific Ltd., and found to be 1.90 μS/cm at room temperature.

2.2. Instrumentation and methods

2.2.1. Stock solution preparation

To ensure adequate homogeneity, a DNA stock solution was prepared by dissolving an appropriate DNA quantity in Trizma buffer solution and then kept it at 4 °C for over a day while being moderately shaken. The determination of DNA concentrations in solutions was determined using a UV–vis spectrophotometer, employing an extinction coefficient of 13,200 M^{-1} cm^{-1} at a 260 nm wavelength. The resulting values were represented in terms of base molarity. At 260 nm/280 nm, the DNA stock solution's absorbance ratio was determined to be 1.87, suggesting a lack of proteins and sufficient purity for further investigations [13,14]. All other stock solutions (e.g., trazodone hydrochloride, ethidium bromide, sodium chloride, etc.) were prepared in HPLC-grade water.

2.2.2. UV–visible absorption spectroscopy

UV–vis spectra of free trazodone and its complex with DNA were obtained from a UV 1900i double beam spectrophotometer (Shimadzu, Japan) by using quarts cuvettes with a 10 mm path length at ambient temperature. Stock solution of trazodone was diluted in HPLC-grade water and spectra were measured between 200 and 600 nm wavelength region. Trazodone at a constant concentration (40 μM) was titrated against DNA's various concentrations (10–80 μM), and alteration in absorbance of trazodone upon interaction with DNA was measured.

2.2.3. DNA denaturation study

Experiments on DNA denaturation was conducted by measuring DNA absorbance (80 μM) at 260 nm with (80 μM) and without trazodone, at various temperatures (20–100 °C) utilizing Jasco V-780 UV–Visible/NIR spectrophotometer (Jasco International Co. Ltd., Hachioji, Japan) with a thermocouple. Using a thermocouple connected to the sample holder, the sample's temperature was measured. For both systems (DNA and trazodone-DNA), the absorbance ratio (A) at a specific temperature to absorbance at 25 °C with temperature has been plotted. DNA's melting temperature, or Tm, has been determined to be the midpoint of both lower and higher inflection points of the melting curve transition. First derivative plot was also plotted from the melting curve and Tm was calculated as the peak of maxima.

2.2.4. Fluorescence spectroscopy investigations

All fluorescence investigations, except time-resolved fluorescence studies, were performed utilizing a Horiba Fluorolog®-3 spectrofluorometer (Jobin Yvon, Horiba) coupled with a flash lamp of xenon and 1 cm rectangular quartz cuvettes.

2.2.4.1. Steady-state and time-resolved fluorescence. Trazodone emission spectra were collected in the wavelength between 330 and 600 nm after excitation at 320 nm with the widths of the excitation and emission slits adjusted to 4 nm bandpass. By titrating a constant volume of trazodone (40 μM) with DNA concentrations that varied from 0.1 to 1.0 μM, an alteration in the fluorescence intensity was noticed. Fluorescence lifetimes were measured using the Time-Correlated Single-Photon Counting (TCSPC) method on an Edinburg FL 900 fluorescence spectrophotometer (Photonics Division, Edinburg Instruments) using a Xenon arc lamp as an excitation source. A picosecond pulse diode laser source having a wavelength of 375.8 nm with a pulse width of 73.5 ps is utilized. The decays were deconvoluted on the FAST (Fluorescence Analysis Software Technology) software package, Edinburgh Instruments.

2.2.4.2. Dye displacement assays. In the ethidium bromide (EtBr) assay, an emission spectrum of 2 μM EtBr alone was obtained. Moreover, 2 μM EtBr was added to 40 μM DNA solution, and emission spectra were obtained in the 486–750 nm wavelength region while excited at 476 nm. This EtBr-DNA mixture was further titrated with various concentrations

of trazodone (0.1–0.8 μM) to assess its capability to displace EtBr.

Similarly, in another experiment, rhodamine B (RB) displacement was performed. In this assay, fluorescence spectra of RB alone (0.5 μM) and RB-DNA complex (0.5 μM–40 μM) were acquired between the range of 562–800 nm wavelength while exciting at 552 nm. To investigate its potential to displace RB, this RB-DNA combination was titrated with increasing concentrations of trazodone.

2.2.4.3. Role of electrostatic interaction. Using sodium chloride, the impact of ionic strength or electrostatic interaction on the trazodone-DNA complex was examined. The experiment was performed by regulating the sodium chloride concentration from 0 to 80 mM in a solution having 40 μM trazodone and 40 μM DNA. Emission spectra were collected ranging from 330 and 600 nm wavelength when trazodone-DNA was excited at 320 nm.

2.2.5. Circular dichroism spectroscopy

Circular dichroism (CD) spectra of DNA (80 μM) without and with trazodone (20–80 μM) were obtained with a J-1500 CD spectrophotometer (Jasco Int. Co. Ltd., Japan). Each CD spectra were collected at a 200–350 nm wavelength range utilizing a cuvette of quartz with a 10 mm path length. Dry nitrogen was implemented to deoxygenate the CD spectrometer's optical chamber before it was utilized, and it was maintained in a nitrogen atmosphere throughout the experiment. Each spectrum comprised the average of three independent scans performed at a speed of 100 nm/min at 25 °C. Baseline corrections were implemented accordingly throughout the experiment.

2.2.6. Molecular docking

Molecular docking was conducted using AutoDock 4.2 software [15] to investigate how TZD binds with DNA Duplex using the Lamarckian Genetic Algorithm [16]. The 3D structure of TZD was drawn using ChemDraw ultra 14.0 software, and the energy minimisation of the structure was done using ChemDraw ultra 3D 14.0. while the crystal structure of DNA was obtained from the Protein Data Bank (PDB ID: 1BNA) [17]. MGL Tools were utilized to prepare coordinate (PDBQT format) and parameter files for TZD and DNA. A grid box measuring 20 × 20 × 20 Å with a grid point spacing of 0.375 Å was created to encompass the entire DNA and facilitate ligand movement. The box centre was set at15 × 19 × 9. Docking parameters were configured to generate 100 poses and these poses were subsequently analyzed for stable interactions using Biovia Discovery Studio Visualizer, and chimera softwares [18].

2.2.7. Molecular dynamic simulation

Molecular Dynamics Simulations (MDS) were conducted using NVIDIA GeForce Gaming RTX 12GB GDD R6X. The docked pose with the lowest binding affinity served as the initial geometry for MD Simulation. Structure and coordinate files for both TZD and DNA were prepared using Gromacs 22.2 [17]. The SPC solvent model was selected for Molecular Dynamics (MD), and a triclinic box measuring 32 × 48 × 48 Å was utilized for the complex. Sodium and chloride ions were introduced to neutralize the system based on total charges. To achieve energy minimization, the steepest descent algorithm was employed over 5000 steps. The MD simulations were conducted under NVT/NPT conditions (300 K, 1 bar) with the presence of 0.15 M NaCl. The simulation was configured to produce 1000 frames, running for a total simulation time of 100 ns and utilizing 50 cycles. Default settings were maintained for all other parameters.

3. Results and discussion

3.1. UV–vis absorption spectroscopy investigation

For analyzing the interaction among DNA and small molecules, UV–vis absorption spectroscopy is the most commonly utilized analytical technique owing to its simplicity and efficiency. The UV-electronic absorption spectrum is useful for demonstrating the affinity of the drug, the structural alterations of DNA caused by the drug, and the binding mechanism [19]. Prior research has documented that the interaction between a ligand and DNA may lead to the formation of a complex, that subsequently has the potential to induce a shift in absorbance toward either red or blue [20,21]. A significant redshift of over 10 nm and hypochromicity of up to 40 % are characteristics of the intercalation binding mode. Redshift in the absorption band is recognized as an outcome of coupling between the binding molecule's π* orbital and the DNA base pair's π orbitals. In contrast, the external and groove binding interactions are visually depicted through a slight spectral shift accompanied by an intermittent hyperchromic effect [22].

The experiment was conducted using a fixed concentration of trazodone and progressively increasing DNA concentrations, as illustrated in Fig. 2 (a). Hyperchromism with bathochromic or redshift was found in the absorption spectra of trazodone as the concentration of DNA increased. Although a rise in absorbance was noticed, therefore, intercalative binding between trazodone and DNA is eliminated and minor groove binding among trazodone and DNA is proposed. Furthermore, the bathochromic shift suggests the stability of the TZD-DNA complex. Ikhlas et al. reported similar types of findings when they studied the interaction between DNA and guggulsterone (a plant-based sterol) [23].

To compute the binding constant of the molecule with DNA, the subsequent Eq. (1) was utilized [17]:

$$\frac{1}{A - A_0} = \frac{1}{A_0} + \frac{1}{KA_0[DNA]} \tag{1}$$

where, A and A_0 indicate the drug's absorbance with and without DNA, respectively. The binding constant of trazodone with DNA is denoted by K. As depicted in Fig. 2 (b), it was observed that the plot between 1/(A-A_0) and 1/[DNA] followed a linear trend. Moreover, it was found that the TZD-DNA complex has a binding constant of $K = 1.32 \times 10^4\ M^{-1}$.

3.2. DNA melting analysis

Base stacking and hydrogen bonding interaction contribute to the outstanding stability of DNA's double-helical strands. When temperature rises, distinct binding forces become weakened, causing double-helical strands to separate into single strands. It was determined as the melting temperature (Tm) of DNA when 50 % of the double-helical DNA helix unfolds and produces two separate strands. The interaction of DNA with small molecules is well known in terms of Tm value. The Tm is enhanced by around 5–8 °C when small molecules are bound to double helix DNA through the intercalative binding mechanism. Non-intercalative interaction, which includes groove binding or electrostatic interaction, induces no or little alteration in Tm [24].

The Tm measurement for DNA with several concentrations of trazodone and without trazodone was obtained by plotting $A/A_{25°C}$ with temperature and measuring absorbance at 260 nm. In this case, absorbance at 25 °C is represented by $A_{25°C}$, while absorbance at temperatures that vary from 25 °C to 102 °C is represented by A. The Tm for both systems (DNA, DNA-TZD) transition was calculated by taking the melting curve's transition midpoint. The DNA melting profiles of DNA with and without trazodone are displayed in Fig. 3. First derivative curve was also obtained and shown in Fig. 3 inset. First derivation of the melting point curve obtained first in Fig. 3 inset, helps to easily pin point the melting temperature of DNA dissociation. The maxima of the derivation curve represent the melting temperature of DNA and DNA-TZD, which were ≈94 °C and ≈95 °C respectively. Such shifting in Tm may be due to an alteration in DNA conformation caused by trazodone groove interaction with DNA, implying non-intercalative binding of trazodone to DNA. This can be comprehensibly explained by the fact that the hydrogen bond interactions between the DNA base pairs are

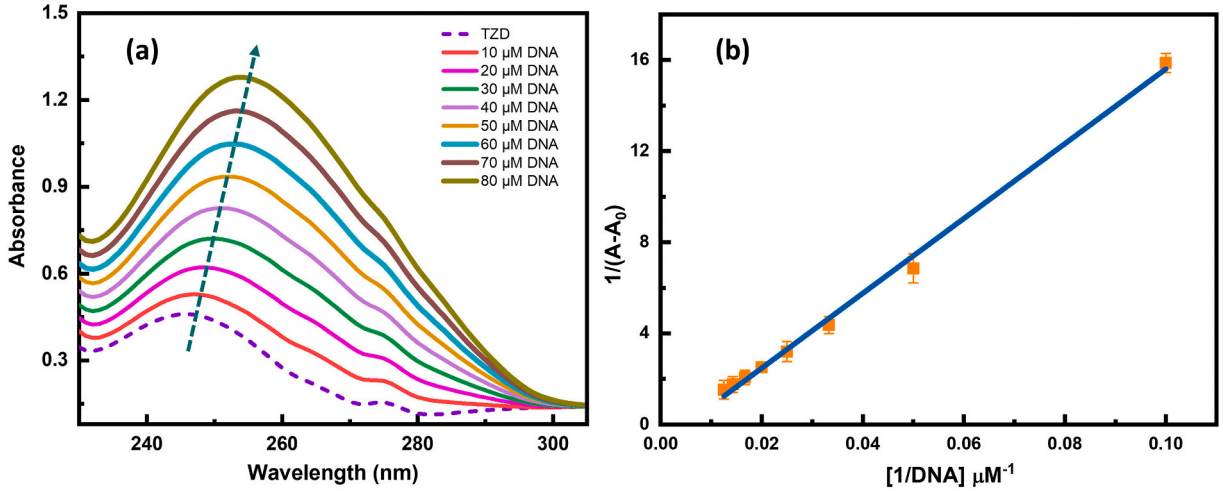

Fig. 2. (a) UV–visible spectra of trazodone with (10–80 μM) and without DNA. (b) Double reciprocal plot of trazodone and DNA.

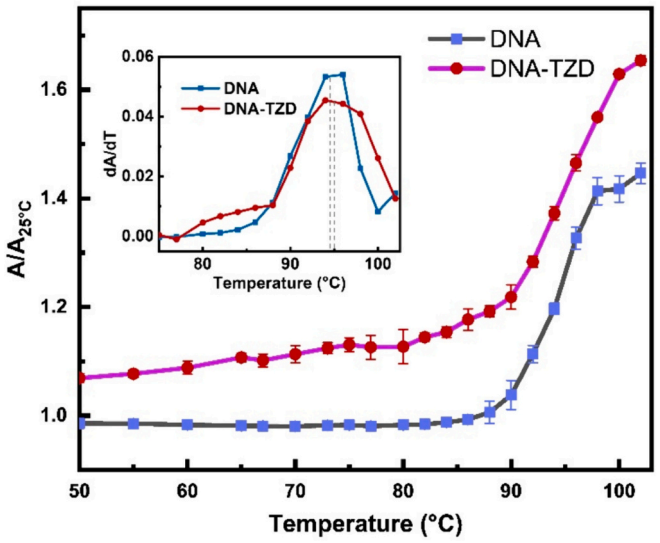

Fig. 3. DNA thermal melting profile in the absence and presence of trazodone and inset shows derivative melting curve of DNA and DNA-TZD.

ruptured along with the melting of the DNA helix. This process is only nominally influenced by the groove or electrostatic binding of small molecules to DNA [25]. Qumaizi et al. reported similar slight alterations in the Tm value of DNA and the antidiabetic drug pioglitazone [26]. Another interaction study between pirenzepine, a drug that treats gastrointestinal disorders, and DNA was performed by Rahman and co-workers. They observed ≈2 °C shift in the Tm values of DNA-pirenzepine and DNA, hence proposed an interaction mechanism involving groove binding [27].

3.3. Steady-state and time-resolved fluorescence analysis

Fluorescence spectroscopy is a remarkably efficient and exceptionally perceptive technique utilized for the purpose of monitoring the drug-DNA binding processes. The present study utilized fluorescence emission spectroscopy to assess binding parameters. A concentration-dependent quenching in trazodone fluorescence was noticed upon titrating trazodone with enhancing DNA concentration, indicating the presence of an interaction among them. DNA has an extremely faint fluorescence signal, so the fluorescence properties of trazodone were utilized. Excitation of trazodone at 320 nm produced a fluorescence emission peak at approximately 445 nm, as illustrated in Fig. 4 (a).

Fluorescence quenching influences the intensity of fluorescence emitted by a fluorophore. Quenching denotes a reduction in intensity caused by interactions that facilitate non-radiative decay. The conventional quenching process is generally governed by the linear Stern-Volmer Eq. [28]:

$$\frac{I_0}{I} = 1 + K_{sv}[Q] = 1 + k_q \tau_0 \, [Q] \tag{2}$$

Here, I and I_0 represent the solute molecules' fluorescence intensity when there is a quencher present and when there is no quencher, respectively. The quencher's molar concentration is represented by [Q], τ_0 is the fluorescence lifetime of the fluorophore without quencher, kq is the rate constant of bimolecular quenching, and the Stern-Volmer quenching constant, or K_{SV}, can have many interpretations based on the mechanism by which quenching occurs.

Quenching occurs through two distinct mechanisms: dynamic and static. The fundamental prerequisite for both types of quenching is the molecular connection of the fluorophore with the quencher. The system under study has nonlinear relative fluorescence intensity versus [Q] Stern-Volmer plots as shown in Fig. 4 (b) that exhibit negative deviation (downward curvature) at higher quencher concentrations (0.1–1.0 μM). The deviation from linearity is usually described as the quenching process regulated by the simultaneous behavior of static and dynamic quenching. When the Stern-Volmer plot shows linearity, the interaction can only be either dynamic or static [29,30]. At this point, the time-resolved fluorescence decay approach has been employed to investigate the mechanistic understanding of the detected fluorescence quenching. Fig. 4 (c) illustrates the typical nanosecond-resolved fluorescence decay profile of trazodone in the presence of varying DNA concentrations, while Table 1 provides the pertinent decay parameters. The expression presented below describes the multiexponential fluorescence decay (I(t)) [31,32]:

$$I(t) = \sum_i^n \alpha_i exp\left(\frac{-t}{\tau_i}\right) \tag{3}$$

Here, α_i denotes the pre-exponential factor (amplitude) that corresponds to the i^{th} decay time constant, τ_i.

The intensity-weighted average lifespan, $\langle \tau_{i0} \rangle$, can be defined as [30,33]:

$$\langle \tau_{i0} \rangle = \frac{\sum_i \alpha_i \tau_i^2}{\sum_i \alpha_i \, \tau_i} \tag{4}$$

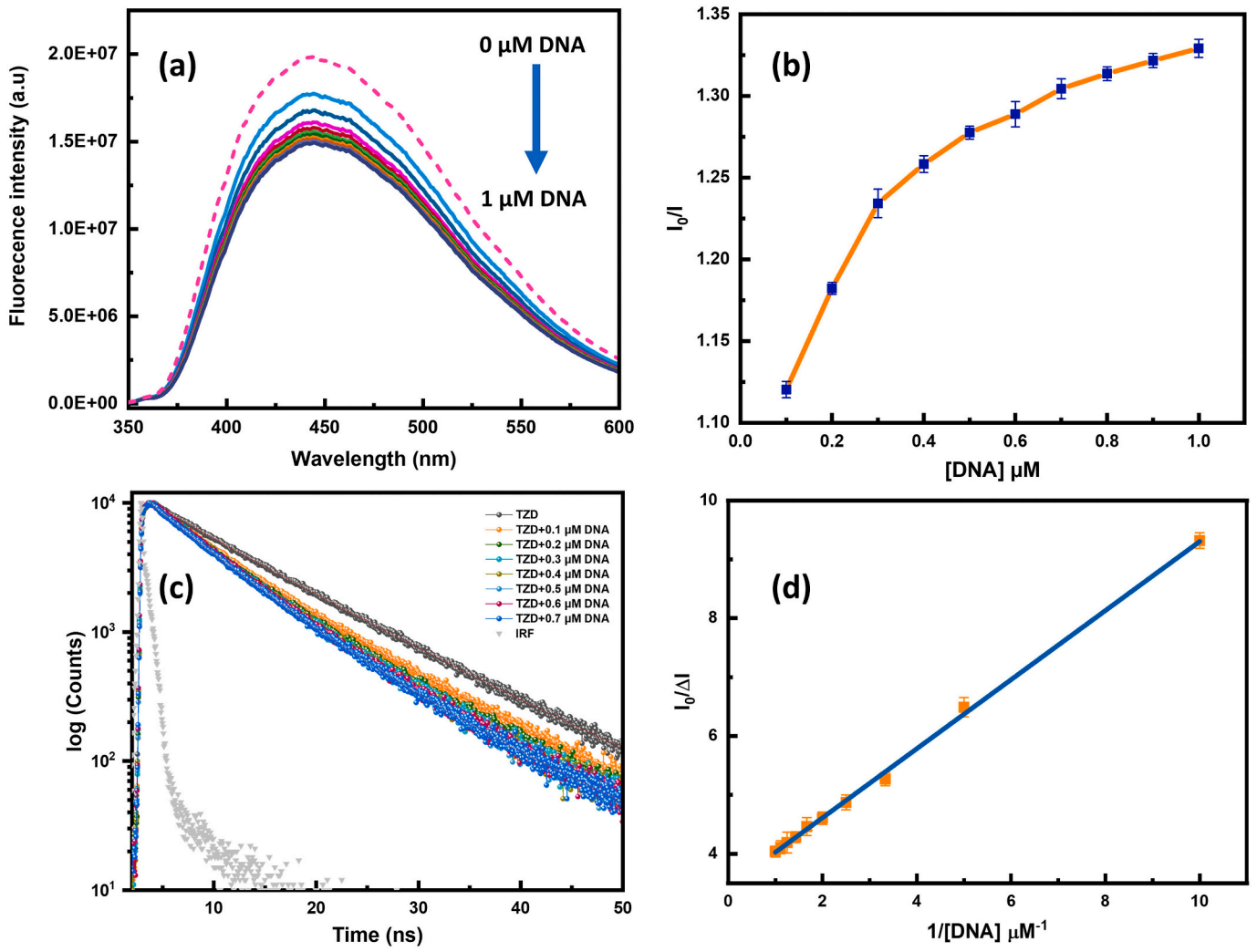

Fig. 4. (a) Steady-state emission spectra of trazodone without and with increasing DNA concentration (0.1–1.0 μM). (b) Nonlinear relative fluorescence intensity versus concentration of DNA graph. (c) Time-resolved fluorescence decay profiles (λ_{ex} = 375 nm, $\lambda_{monitored} = \lambda_{em}^{max}$) of trazodone with varied DNA concentrations. (d) Linear plots of I_0 / ΔI versus 1/[Q].

Table 1
Time-resolved fluorescence decay parameters of trazodone in the presence of varying DNA concentrations (λ_{ex} = 375 nm, $\lambda_{monitored}$ = 445 nm).

Sample	τ_1 (ns)	τ_2 (ns)	α_1 (%)	α_2 (%)	τ_{i0} (ns)	τ_{a0} (ns)	χ^2
TZD alone	5.97 ± 1.02	10.68 ± 0.33	10.49	89.51	10.39	10.19	1.07
TZD + 0.1 μM DNA	5.19 ± 0.21	10.18 ± 0.25	27.69	72.31	9.36	8.80	1.14
TZD + 0.2 μM DNA	6.00 ± 0.18	11.31 ± 0.63	54.05	45.95	9.27	8.44	1.06
TZD + 0.3 μM DNA	5.50 ± 0.20	9.87 ± 0.39	43.27	56.73	8.57	7.98	1.11
TZD + 0.4 μM DNA	5.34 ± 0.21	9.46 ± 0.33	39.56	60.44	8.35	7.83	1.09
TZD + 0.5 μM DNA	5.90 ± 0.17	10.85 ± 0.65	58.34	41.66	8.71	7.96	1.06
TZD + 0.6 μM DNA	5.68 ± 0.18	10.39 ± 0.54	52.61	47.39	8.61	7.91	1.13
TZD + 0.7 μM DNA	5.75 ± 0.17	10.53 ± 0.57	55.66	44.34	8.59	7.87	1.05

and an amplitude-weighted average lifetime $\langle\tau_{a0}\rangle$, as [30,33]:

$$\langle\tau_{a0}\rangle = \frac{\sum_i \alpha_i \tau_i}{\sum_i \alpha_i} \quad (5)$$

Data from Table 1 shows that the presence of a lower concentration of DNA substantially perturbs both the intensity-weighted and amplitude-weighted average lifetimes of trazodone. The possibility of a static quenching process is negated by the reasonable inconstancy of trazodone average lifetime with lower quencher (DNA) concentrations (for static quenching, $\tau_0/\tau = 1$). Therefore, based on the fluorescence decay trend of trazodone as a function of varying concentrations of DNA actuating the mechanism of fluorescence quenching can be rationalized as dynamic at lower DNA concentration [32,34,35] The Stern-Volmer graphs are explained by diffusion-restricted dynamic quenching and seem to be linear in the lower concentration level. Any one of the two causes might be the cause of the plot's negative deviation. The first is the existence of two fluorophores with varying quencher accessibility. Second, fluorophores are part of a ligand's binding site that functions like a quencher and are easily quenched, but fluorophores that are not part of the binding might not be quenched at all. The plot of Stern-Volmer shows a negative deviation to linearity due from a diverse

population of fluorophores. The modified "Stern–Volmer" or Lehrer equation, which is provided below, can be used to express quenching information that is anticipated to result from one of these causes [36]:

$$I = (1-f)I_0 + \frac{fI_0}{1+K_{sv}[Q]} \quad (6)$$

Another way to express the above equation in linear form is as follows:

$$\frac{I_0}{\Delta I} = \frac{1}{f} + \frac{1}{fK_{sv}[Q]} \quad (7)$$

In this case, $\Delta I = I_0 - I$. As depicted in Fig. 4 **(d)** a linear plot of $I_0/\Delta I$ Vs 1/[Q] is observed where $1/f$ acts as the intercept and K_{SV} equals to intercept/slope. K_{SV} was determined to be 5.84 ($\pm$0.012) $\times$ 10^6 M^{-1} with a value of f smaller than 1. As the magnitude of K_{SV} increases, the quenching becomes more effective, resulting in a higher degree of exposure of the quencher to the probe [32]. The value of the bimolecular quenching rate parameter (kq) is determined by using the formula $kq = K_{SV}/\tau_0$ which is derived from Eq. (2) and found to be 5.73 $\times$ 10^{14} M^{-1} s^{-1}. K_{SV} is obtained from Eq. (7), and τ_0 is the lifetime of the fluorophore when there is no quencher present. Higher kq values indicate that fluorescence is quenched more efficiently [36]. A bimolecular quenching constant that is greater than the maximum possible value indicates the absence of a pure collisional process, and the quenching could be a result of mixed quenching and static quenching [37].

3.4. Dye displacement assay

To decipher the drug-DNA binding manner of interaction, several well-known fluorescent dyes with clearly implemented binding modes are used. In competitor deracination attempts, any small molecule capable of replacing the dye that was previously bound to DNA will exhibit a similar interaction mode with DNA as the substituted dye. The alteration in fluorescence intensity of the drug-DNA combination upon drug accession provides significant insights into the mode of binding [38]. Similar displacement approaches were utilized to study the interaction of various compounds with DNA [39,40].

Ethidium bromide binds to DNA as an intercalative dye. Therefore, EtBr functions as an efficient spectrum probe in the investigation of drug-DNA binding. When EtBr is isolated in solution, it exhibits a faint fluorescence; however, upon intercalation with DNA, its fluorescence becomes considerably more pronounced. Since it does not emanate visible light in the aqueous condition after being quenched by a solvent, EtBr is frequently utilized in binding studies of DNA for recognizing the binding mode. DNA intercalation significantly amplifies the emission of EtBr. EtBr is displaced by drugs that bind through DNA intercalation, resulting in a diminution in the EtBr-DNA complex fluorescence intensity [41]. It is evident from Fig. 5 **(a)** that there was no discernible alteration in fluorescence intensity with subsequent variations in trazodone concentration; this indicates that trazodone lacks the ability to exchange EtBr. This result confirmed the existence of a minor groove binding probability and the non-intercalative binding. Therefore, to ensure the probability of minor groove interaction, a further dye

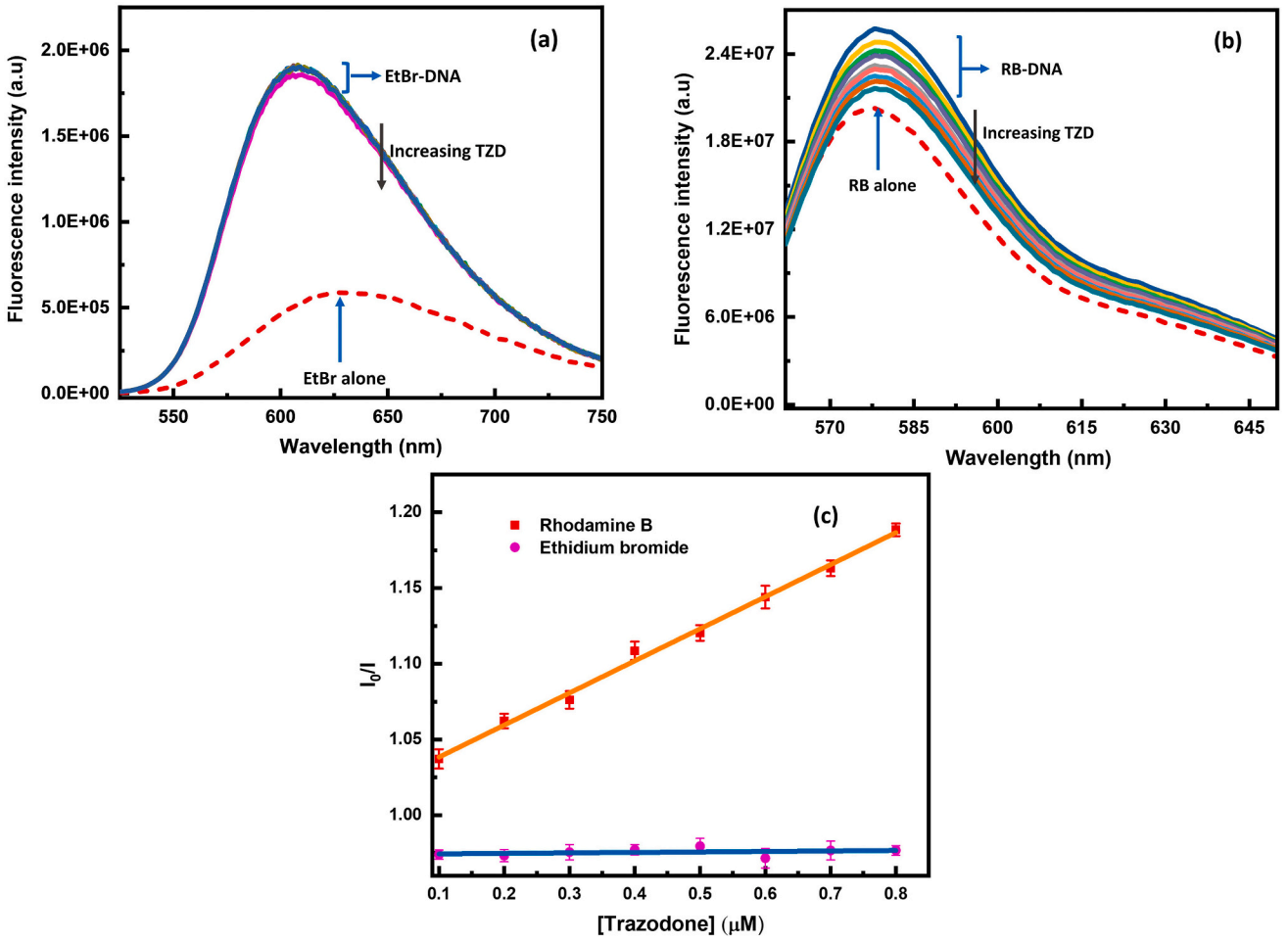

Fig. 5. Competitive emission spectra between trazodone and: (a) EtBr, (b) Rhodamine B, (c) Relative fluorescence intensity of rhodamine B and EtBr dyes with DNA complex as trazodone concentration increases.

displacement experiment was performed by employing a commonly known minor groove binder.

Rhodamine B is a fluorescent dye that is often recognized as a minor groove-binding dye. Rhodamine B emits mild fluorescence when alone, but the intensity increases dramatically when attached to DNA. Subsequently, the fluorescence intensity produced by the RB-DNA combination will diminish as a result of the displacement of RB by drugs that bind to DNA at the minor groove site [23]. The reduction in fluorescence intensity observed in Fig. 5 **(b)** in response to a subsequent increase in trazodone concentration indicates that trazodone displaces RB. This drop in fluorescence intensity verifies that trazodone interacts with DNA via a minor groove. [42] The relative fluorescence intensity of EtBr and RB bound to DNA with increasing the concentration of trazodone is depicted in Fig. 5 **(c)**.

3.5. Ionic interaction analysis

The electrostatic interaction mode, a type of the drug molecule's non-covalent interaction modes on DNA, is a preferred auxiliary mechanism for groove and intercalation binding. The differentiation of small molecule-DNA binding modes can be accomplished effectively by observing the spectral shift caused by varying ionic strengths. Sodium chloride was utilized to evaluate any ionic interaction between DNA and drug in the current experiment [25,42]. The presence of NaCl in a system result in a decrease in electrostatic repulsion between adjacent nucleotides that have negatively charged phosphate backbones as the concentration of Na^+ increases. Therefore, an increase in the medium's ionic strength will result in a weakening of the electrostatic interaction between fluorophore and DNA. The electrostatic interaction between the drug and DNA decreases when an electrolyte like NaCl is titrated to a drug-DNA solution, resulting in the discharge of the drug into the solution [13,43].

The fluorescence emission spectra of the trazodone-DNA combination were investigated to determine the ionic interaction among them using NaCl (Fig. 6 **a**). In the presence of varying concentrations of NaCl in the solution of DNA and trazodone complex, the fluorescence intensity showed a negligible alteration. The findings indicate that the binding of trazodone with DNA is not significantly affected by the increase in cathodic ion strength and therefore negligible involvement of ionic forces. The plot of relative fluorescence intensity (I_0/I) with various concentrations of NaCl was found to be linear as shown in Fig. 6 **(b)** and a visual representation of the pattern of variation is given by the solid line. Various other drugs like cefotaxime (a third-generation antibiotic) [43], Cu (II) complex of isoxsuprine (a vasodilating drug for humans and equine) [44] and tepotinib (anticancer medicine) [45] also show similar results with NaCl and suggested negligible effect on DNA-drug complex.

3.6. Circular dichroism analysis

This is an effective approach for detecting modifications to the secondary conformation of DNA, which is involved in small-molecule interactions [46]. The CD-spectra of B-form of DNA demonstrates a positive signal at about 276 nm, corresponding to the base stacking, and a negative signal at around 247 nm, attributed to right-handed helicity, in a buffer (pH 7.4) solution that is the characteristics of the typical B-form (right-handed) of DNA in buffer solution [2,47]. These peaks are susceptible to the binding of any small molecule or drugs, therefore variations in DNA's CD signals noticed during drug interaction may typically be attributed to modifications in the structure of DNA. [48] Electrostatic and simple groove binding of DNA with small molecules produces minimal or no disturbance to the helicity bands and base stacking, whilst intercalation raises band intensities and stabilizes the B form of DNA as shown with conventional intercalator methylene blue [49].

The impact of trazodone on the structure of DNA is assessed by CD spectroscopy and the results are displayed in Fig. 7. In the current study, the CD spectra of DNA without and with trazodone (20–80 μM) show negligible variations in the intensity of both positive and negative peaks with no significant modifications suggesting a groove-binding mode of interaction. These findings are already confirmed by the UV–vis

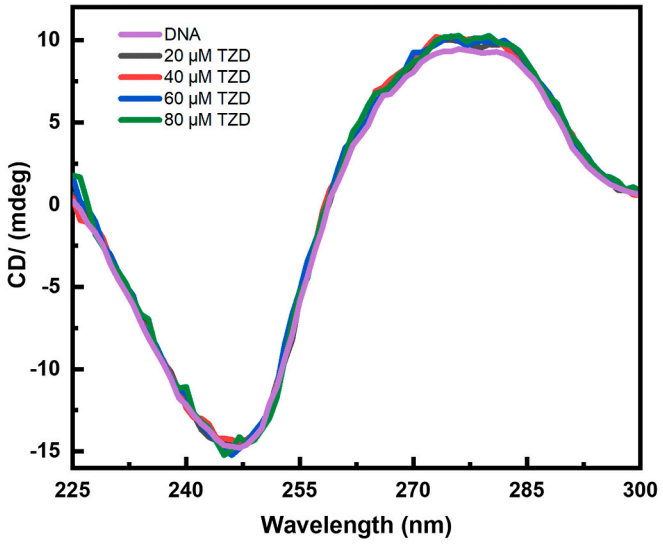

Fig. 7. CD spectra of free DNA (80 μM) in Trizma buffer solution (pH 7.4) with various concentrations of trazodone (20–80 μM) in DNA.

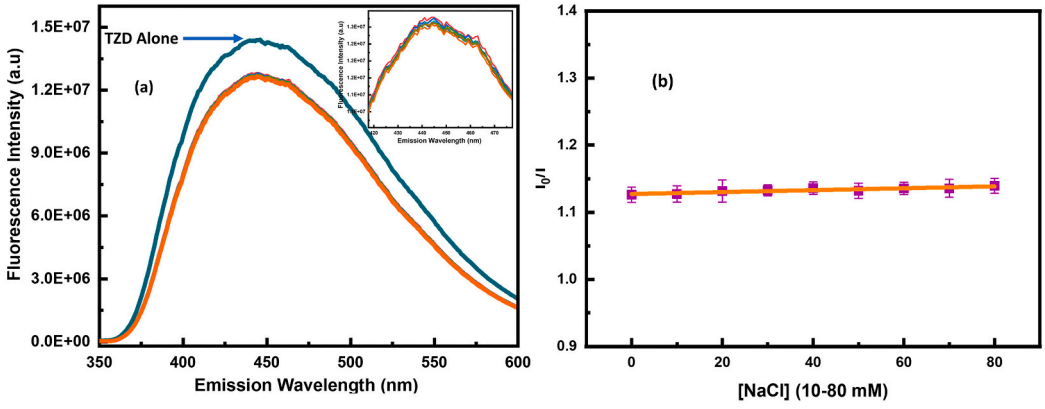

Fig. 6. (a) Emission spectra of trazodone and trazodone-DNA complex (inset) in the presence of different concentrations (10–80 mM) of NaCl and (b) relative variation of trazodone fluorescence intensity (I_0 is the fluorescence intensity without NaCl; I/I_0 at $\lambda_{em} \approx 445$ nm) (±1 % error associated with each parameter).

spectroscopy study and dye displacement assay. This finding also agrees with that of Husain et al. which revealed that the groove-binding drug cannot perturb base pair stacking and conformation of DNA [50]. Furthermore, our results are in line with those of Yasmeen et al., who also found comparable results between DNA and the medication thalidomide [41].

3.7. Molecular docking

Molecular Docking provides insights into how ligands interact with macromolecules [51]. The results revealed 100 poses clustered into 9 distinct groups, predominantly in the minor groove, indicating a preference for binding in this region of DNA (Fig. 8). The pose with the highest binding affinity, −8.0877 kcal/mol, was selected for further Molecular Dynamics Simulation (MDS) analysis. Trazodone was observed to interact with the minor groove through its amine group, via van der Waal interaction in the phosphate backbone of adenine and thymine in the chain S. Additionally, the part of the trazodone, aromatic group, engaged in pi-alkyl interactions with the pyrimidine ring of adenine (chain A) (Fig. 8 c). The complex formation was further stabilized by significant van der Waals contacts.

3.8. MD simulation

MD simulation from GROMACS 2023.2 was performed for the best poses selected from the docking studies. RMSD as a function of time is plotted for all the complexes in Fig. 9 to obtain the systematic deviation of complexes [15]. The RMSD profile shows that the ligands, trazodone remain bound to the DNA near the preferential binding site. Molecular Dynamics Simulations were conducted to assess the stability of the TZD-DNA complex over a period of 100 ns in a solvent environment. The starting structure for the simulations was chosen based on the docked pose with the highest binding affinity. Throughout the simulation, the RMSD of the TZD-DNA complex remained relatively stable, showing only minor fluctuations with an average RMSD of 0.3–0.4 nm (Fig. 9 (a)). During the trajectory, trazodone initially moved from the minor groove to the major groove at 40 ns and stayed there until 60 ns. Afterward, trazodone reverted to the minor groove and remained stable for the rest of the simulation. The RMSF shown in Fig. 9 (d) was found to be decreased from 1.0 to 0.5 nm in case of complex which suggests there is lesser fluctuation in the TZD-DNA complex as compared to the DNA which reveals the stability of the complex formed [51]. Also, slight fluctuation was seen at around 12 residue this may be due to internal rotation of the DNA strand [17]. The Rg value was found to be stable over the course of MD run. The Rg value for both complex and DNA was similar suggesting the stability of the complex again. Fig. 9 (c) suggested that there was the involvement of hydrogen bonding, and the number was found to be 3 which corroborate with the results obtained from molecular docking.

4. Conclusion

In the current study, we evaluated the interaction of trazodone with DNA under physiological conditions, utilizing UV–vis absorption, steady-state fluorescence, dye displacement experiment, ionic strength study, circular dichroism, and DNA melting analysis. UV–vis absorption investigations demonstrated that DNA readily interacts with trazodone and contains a binding constant in the 10^4 M^{-1} range. The findings of steady-state fluorescence suggest that trazodone binds with DNA and Stern-Volmer constant is found to be 5.84×10^6 M^{-1}. There are no noticeable alterations in Tm value suggesting that trazodone-DNA interactions are non-intercalative. The outcomes of the competitive binding experiment show that trazodone binds with DNA in a minor groove. The mode of interaction is further corroborated by circular

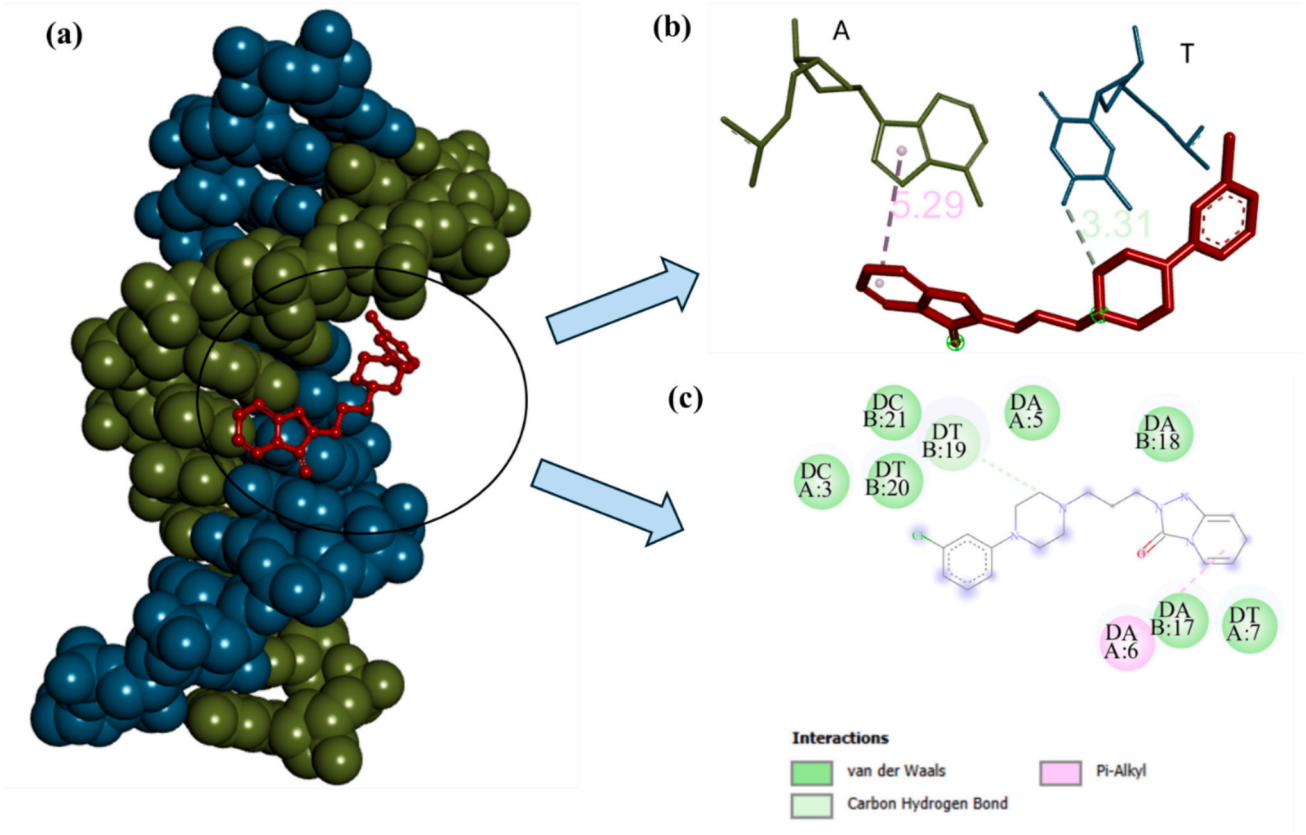

Fig. 8. A molecular docked model for trazodone with DNA (PDB ID: 1BNA). (a) 3D full view of docking between trazodone and DNA (b) The binding mode between trazodone and DNA (c) 2D representation of the interactions between TZD-DNA complex.

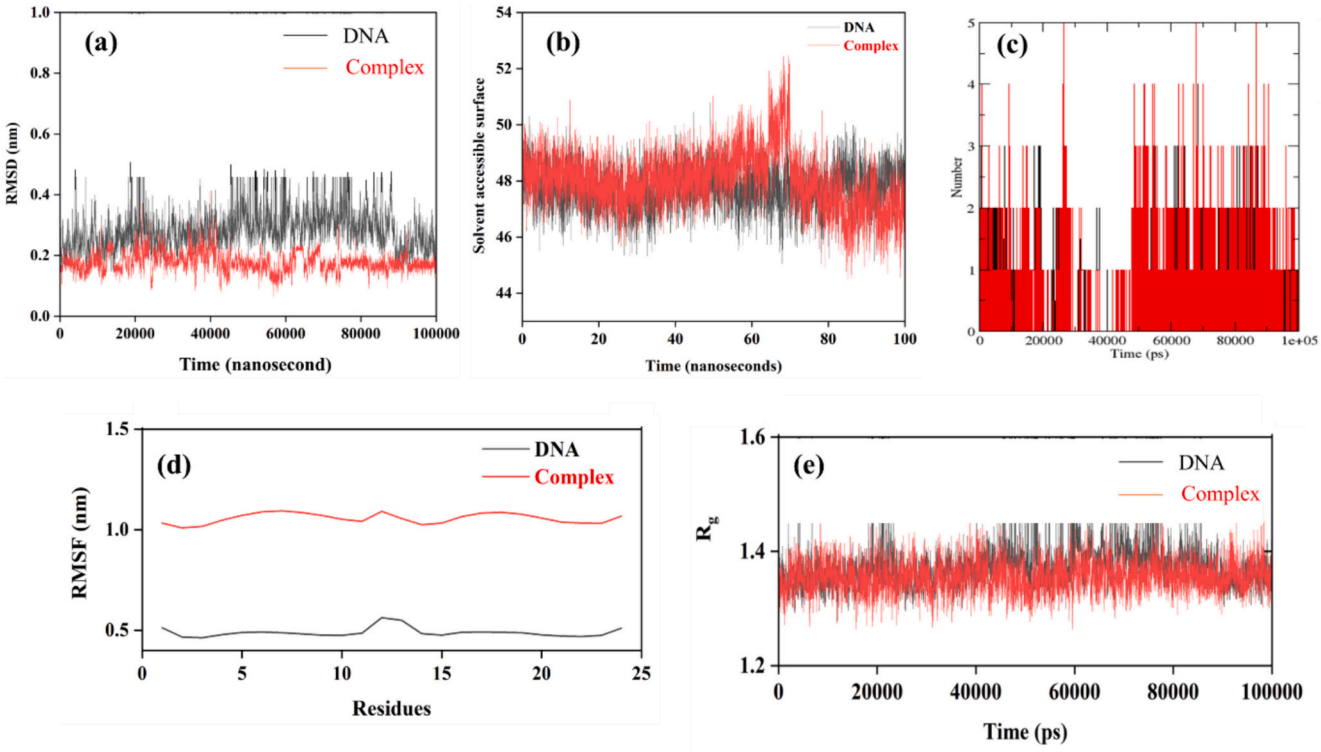

Fig. 9. (a) Root mean square deviation of the backbone of the DNA and docked complex (b) Solvent accession surface (c) no. of H-bond in the complex (d) Root mean square fluctuation of the backbone atoms of the DNA and docked complex (e) Radius of gyration of the DNA-TZD complex generated from 100 ns MD simulations trajectory.

dichroism which showed no significant modifications in DNA confirmation by the binding of trazodone suggesting the groove-binding interaction mode instead of intercalation. In the presence of DNA, the emission intensity of trazodone is unaltered by enhancing the concentration of sodium chloride indicating there is no substantial electrostatic interaction between trazodone and DNA. Molecular dynamic simulation and molecular docking suggested that the TZD-DNA system was stable, and the mode of binding was minor groove. These research findings certainly enhance researchers understanding of trazodone's binding mechanism to DNA and medication's therapeutical properties as well as the development of more potent pharmaceutical compounds.

CRediT authorship contribution statement

Ambrish Kumar: Writing – original draft, Methodology. **Moumita Saha:** Formal analysis, Data curation. **Juhi Saraswat:** Formal analysis, Software. **Kamalakanta Behera:** Writing – review & editing, Supervision, Conceptualization. **Shruti Trivedi:** Writing – review & editing, Supervision, Project administration, Funding acquisition, Conceptualization.

Declaration of competing interest

The authors declare no competing financial interests or personal relationships that could have appeared to influence the work reported in this paper.

Data availability

Data will be made available on request.

Acknowledgments

Dr. K. Behera acknowledges University of Allahabad for the facilities and funding and Dr. S. Trivedi acknowledges the University Grant Commission (UGC), the Trans-Disciplinary Research Project (No. R/Dev/D/IoE/TDR-Projects-II(Sanction)/2023-24/69599 to 2023-24/69600), the Institute of Eminence (IoE)-Banaras Hindu University for the fundings. Ambrish Kumar and Moumita Saha acknowledges the University Grant Commission (UGC), New Delhi for financial assistance in the form of a Junior Research Fellowship.

References

[1] S. Afrin, Y. Rahman, T. Sarwar, M.A. Husain, A. Ali, Shamsuzzaman, M. Tabish, Molecular spectroscopic and thermodynamic studies on the interaction of anti-platelet drug ticlopidine with calf thymus DNA, Spectrochim. Acta A Mol. Biomol. Spectrosc. 186 (2017) 66–75, https://doi.org/10.1016/j.saa.2017.05.073.
[2] S. Sen, R. Sett, B.K. Paul, N. Guchhait, A spectroscopic deciphering of the differential interaction behavior of alkaloid drugs with native B-DNA and protonated DNA, J. Mol. Liq. 312 (2020) 113426, https://doi.org/10.1016/j.molliq.2020.113426.
[3] Y. Temerk, H. Ibrahim, Electrochemical studies and spectroscopic investigations on the interaction of an anticancer drug flutamide with DNA and its analytical applications, J. Electroanal. Chem. 736 (2015) 1–7, https://doi.org/10.1016/j.jelechem.2014.10.019.
[4] A. Mikocka-Walus, A.C. Ford, D.A. Drossman, Antidepressants in inflammatory bowel disease, Nat. Rev. Gastroenterol. Hepatol. 17 (2020) 184–192, https://doi.org/10.1038/s41575-019-0259-y.
[5] S. Kumar, S. Darshan, T.R. Baggi, Recent advances in analytical techniques for antidepressants determination in complex biological matrices: a review, Int. J. Toxicol. 42 (2023) 352–364, https://doi.org/10.1177/10915818221150779.
[6] Å.M.L. Øiestad, R. Karinen, S. Rogde, S. Nilsen, K.-B. Boye Eldor, G. Brochmann, M. Arnestad, E.L. Øiestad, M.D. Peres, L. Kristoffersen, V. Vindenes, Comparative study of postmortem concentrations of antidepressants in several different matrices, J. Anal. Toxicol. 42 (2018) 446–458, https://doi.org/10.1093/jat/bky030.
[7] V. Bortolotto, F. Mancini, G. Mangano, R. Salem, E. Xia, E. Del Grosso, M. Bianchi, P.L. Canonico, L. Polenzani, M. Grilli, Proneurogenic effects of trazodone in murine and human neural progenitor cells, ACS Chem. Neurosci. 8 (2017) 2027–2038, https://doi.org/10.1021/acschemneuro.7b00175.
[8] A. Fagiolini, A. González-Pinto, K.W. Miskowiak, P. Morgado, A.H. Young, E. Vieta, Role of trazodone in treatment of major depressive disorder: an update, Ann. General Psychiatry 22 (2023) 32, https://doi.org/10.1186/s12991-023-00465-y.

[9] I.M. McIntyre, P. Mallett, R. Stabley, Postmortem distribution of trazodone concentrations, Forensic Sci. Int. 251 (2015) 195–201, https://doi.org/10.1016/j.forsciint.2015.04.009.
[10] P. Şenel, S. Agar, M. Yurtsever, A. Gölcü, Voltammetric quantification, spectroscopic, and DFT studies on the binding of the antineoplastic drug Azacitidine with DNA, J. Pharm. Biomed. Anal. 237 (2024) 115746, https://doi.org/10.1016/j.jpba.2023.115746.
[11] R. Nimal, D. Nur Unal, C. Erkmen, B. Bozal-Palabiyik, M. Siddiq, G. Eren, A. Shah, B. Uslu, Development of the electrochemical, spectroscopic and molecular docking approaches toward the investigation of interaction between DNA and anti-leukemic drug azacytidine, Bioelectrochemistry 146 (2022) 108135, https://doi.org/10.1016/j.bioelechem.2022.108135.
[12] D. Takkella, S. Sharma, J. Vishwakarma, J. Cerezo, L. Martinez-Fernandez, K. Gavvala, Unveiling the interaction modes of Imiquimod with DNA: biophysical and computational studies, J. Photochem. Photobiol. A Chem. 447 (2024) 115190, https://doi.org/10.1016/j.jphotochem.2023.115190.
[13] B.K. Paul, N. Guchhait, Exploring the strength, mode, dynamics, and kinetics of binding interaction of a cationic biological photosensitizer with DNA: implication on dissociation of the drug–DNA complex via detergent sequestration, J. Phys. Chem. B 115 (2011) 11938–11949, https://doi.org/10.1021/jp206589e.
[14] N. Singh, M. Sharma, D. Mondal, M.M. Pereira, K. Prasad, Very high concentration solubility and long-term stability of DNA in an ammonium-based ionic liquid: a suitable medium for nucleic acid packaging and preservation, ACS Sustain. Chem. Eng. 5 (2017) 1998–2005, https://doi.org/10.1021/acssuschemeng.6b02842.
[15] J. Saraswat, S. Kumar, K.A. Alzahrani, M.A. Malik, R. Patel, Experimental and computational characterisation of the molecular interactions between 1-Butyl-1-methyl-pyrrolidin-1-ium bis(trifluoromethanesulphonyl)imide and human serum albumin, ChemistrySelect 8 (2023), https://doi.org/10.1002/slct.202204159.
[16] J. Saraswat, P. Singh, R. Patel, A computational approach for the screening of potential antiviral compounds against SARS-CoV-2 protease: ionic liquid vs herbal and natural compounds, J. Mol. Liq. 326 (2021) 115298, https://doi.org/10.1016/j.molliq.2021.115298.
[17] P. Sharma, P. Gopi, S. Singh, M.S.S. Rani, P. Pandya, Binding studies of sertraline hydrochloride with CT-DNA using experimental and computational techniques, Spectrochim. Acta A Mol. Biomol. Spectrosc. 300 (2023) 122910, https://doi.org/10.1016/j.saa.2023.122910.
[18] S. Sharma, P. Kumar, R. Chandra, Applications of BIOVIA materials studio, LAMMPS, and GROMACS in various fields of science and engineering, in: Molecular Dynamics Simulation of Nanocomposites Using BIOVIA Materials Studio, Lammps and Gromacs, Elsevier, 2019, pp. 329–341, https://doi.org/10.1016/B978-0-12-816954-4.00007-3.
[19] P. Şenel, S. Agar, V.O. Sayin, F. Altay, M. Yurtsever, A. Gölcü, Elucidation of binding interactions and mechanism of Fludarabine with dsDNA via multispectroscopic and molecular docking studies, J. Pharm. Biomed. Anal. 179 (2020) 112994, https://doi.org/10.1016/j.jpba.2019.112994.
[20] I. Ahmad, A. Ahmad, M. Ahmad, Binding properties of pendimethalin herbicide to DNA: multispectroscopic and molecular docking approaches, Phys. Chem. Chem. Phys. 18 (2016) 6476–6485, https://doi.org/10.1039/c5cp07351k.
[21] A.T.S. Bodapati, R.S. Reddy, K. Lavanya, S.R. Madku, B.K. Sahoo, Minor groove binding of antihistamine drug bilastine with calf thymus DNA: a molecular perspective with thermodynamics using experimental and theoretical methods, J. Mol. Struct. 1301 (2024) 1–12, https://doi.org/10.1016/j.molstruc.2023.137385.
[22] D. Takkella, S. Sharma, J. Vishwakarma, J. Cerezo, L. Martinez-Fernandez, K. Gavvala, Unveiling the interaction modes of Imiquimod with DNA: biophysical and computational studies, J. Photochem. Photobiol. A Chem. 447 (2024) 115190, https://doi.org/10.1016/j.jphotochem.2023.115190.
[23] S. Ikhlas, M. Ahmad, Binding studies of guggulsterone-E to calf thymus DNA by multi-spectroscopic, calorimetric and molecular docking studies, Spectrochim. Acta A Mol. Biomol. Spectrosc. 190 (2018) 402–408, https://doi.org/10.1016/j.saa.2017.09.065.
[24] S.U. Rehman, T. Sarwar, M.A. Husain, H.M. Ishqi, M. Tabish, Studying non-covalent drug–DNA interactions, Arch. Biochem. Biophys. 576 (2015) 49–60, https://doi.org/10.1016/j.abb.2015.03.024.
[25] B.K. Paul, N. Ghosh, S. Mukherjee, Interaction of an anti-cancer photosensitizer with a genomic DNA: from base pair specificity and thermodynamic landscape to tuning the rate of detergent-sequestered dissociation, J. Colloid Interface Sci. 470 (2016) 211–220, https://doi.org/10.1016/j.jcis.2016.02.059.
[26] K.I. Al Qumaizi, R. Anwer, N. Ahmad, S.M. Alosaimi, T. Fatma, Study on the interaction of antidiabetic drug pioglitazone with calf thymus DNA using spectroscopic techniques, J. Mol. Recognit. 31 (2018) 1–10, https://doi.org/10.1002/jmr.2735.
[27] Y. Rahman, S. Afrin, M.A. Husain, T. Sarwar, A. Ali, Shamsuzzaman, M. Tabish, Unravelling the interaction of pirenzepine, a gastrointestinal disorder drug, with calf thymus DNA: an in vitro and molecular modelling study, Arch. Biochem. Biophys. 625–626 (2017) 1–12, https://doi.org/10.1016/j.abb.2017.05.014.
[28] R. Nimal, D. Nur Unal, C. Erkmen, B. Bozal-Palabiyik, M. Siddiq, G. Eren, A. Shah, B. Uslu, Development of the electrochemical, spectroscopic and molecular docking approaches toward the investigation of interaction between DNA and anti-leukemic drug azacytidine, Bioelectrochemistry 146 (2022) 108135, https://doi.org/10.1016/j.bioelechem.2022.108135.
[29] A. Nandy, S. Shekhar, B.K. Paul, S. Mukherjee, Exploring the nucleobase-specific hydrophobic interaction of cryptolepine hydrate with RNA and its subsequent sequestration, Langmuir 37 (2021) 11176–11187, https://doi.org/10.1021/acs.langmuir.1c02123.
[30] B.K. Paul, D. Ray, N. Guchhait, Unraveling the binding interaction and kinetics of a prospective anti-HIV drug with a model transport protein: results and challenges, Phys. Chem. Chem. Phys. 15 (2013) 1275–1287, https://doi.org/10.1039/c2cp42539d.
[31] Y. Li, S. Natakorn, Y. Chen, M. Safar, M. Cunningham, J. Tian, D.D.U. Li, Investigations on average fluorescence lifetimes for visualizing multi-exponential decays, Front. Phys. 8 (2020), https://doi.org/10.3389/fphy.2020.576862.
[32] J.R. Lakowicz, Principles of Fluorescence Spectroscopy, Springer US, Boston, MA, 1999, https://doi.org/10.1007/978-1-4757-3061-6.
[33] K. Santhosh, S. Patra, S. Soumya, D.C. Khara, A. Samanta, Fluorescence quenching of CdS quantum dots by 4-azetidinyl-7-nitrobenz-2- oxa-1,3-diazole: a mechanistic study, ChemPhysChem 12 (2011) 2735–2741, https://doi.org/10.1002/cphc.201100515.
[34] B.K. Paul, N. Ghosh, S. Mukherjee, Binding interaction of a prospective chemotherapeutic antibacterial drug with β-lactoglobulin: results and challenges, Langmuir 30 (2014) 5921–5929, https://doi.org/10.1021/la501252x.
[35] B.K. Paul, N. Ghosh, S. Mukherjee, Binding of norharmane with RNA reveals two thermodynamically different binding modes with opposing heat capacity changes, J. Colloid Interface Sci. 538 (2019) 587–596, https://doi.org/10.1016/j.jcis.2018.12.011.
[36] H.S. Geethanjali, D. Nagaraja, R.M. Melavanki, R.A. Kusanur, Fluorescence quenching of boronic acid derivatives by aniline in alcohols – a negative deviation from Stern–Volmer equation, J. Lumin. 167 (2015) 216–221, https://doi.org/10.1016/j.jlumin.2015.06.040.
[37] S.R. Madku, B.K. Sahoo, K. Lavanya, R.S. Reddy, A.T.S. Bodapati, DNA binding studies of antifungal drug posaconazole using spectroscopic and molecular docking methods, Int. J. Biol. Macromol. 225 (2023) 745–756, https://doi.org/10.1016/j.ijbiomac.2022.11.137.
[38] A. Mukherjee, B. Singh, Binding interaction of pharmaceutical drug captopril with calf thymus DNA: a multispectroscopic and molecular docking study, J. Lumin. 190 (2017) 319–327, https://doi.org/10.1016/j.jlumin.2017.05.068.
[39] A. Subastri, A. Durga, K. Harikrishna, M. Sureshkumar, K. Jeevaratnam, K. S. Girish, C. Thirunavukkarasu, Exploration of disulfiram dealings with calf thymus DNA using spectroscopic, electrochemical and molecular docking techniques, J. Lumin. 170 (2016) 255–261, https://doi.org/10.1016/j.jlumin.2015.10.001.
[40] N. Shahabadi, M. Maghsudi, Multi-spectroscopic and molecular modeling studies on the interaction of antihypertensive drug; methyldopa with calf thymus DNA, Mol. BioSyst. 10 (2014) 338–347, https://doi.org/10.1039/C3MB70340A.
[41] S. Yasmeen, F.A. Qais, M. Rana, A. Islam, Rahisuddin, Binding and thermodynamic study of thalidomide with calf thymus DNA: spectroscopic and computational approaches, Int. J. Biol. Macromol. 207 (2022) 644–655, https://doi.org/10.1016/j.ijbiomac.2022.03.036.
[42] T. Sarwar, S.U. Rehman, M.A. Husain, H.M. Ishqi, M. Tabish, Interaction of coumarin with calf thymus DNA: deciphering the mode of binding by in vitro studies, Int. J. Biol. Macromol. 73 (2015) 9–16, https://doi.org/10.1016/j.ijbiomac.2014.10.017.
[43] F.A. Qais, I. Ahmad, In vitro interaction of cefotaxime with calf thymus DNA: insights from spectroscopic, calorimetric and molecular modelling studies, J. Pharm. Biomed. Anal. 149 (2018) 193–205, https://doi.org/10.1016/j.jpba.2017.10.016.
[44] F. Hajibabaei, S. Salehzadeh, R. Golbedaghi, N. Hosseinpour, S. Sharifinia, S. Khazalpour, Z. Baghaeifar, DNA binding and molecular docking studies of a new Cu (II) complex of isoxsuprine drug, Polyhedron 162 (2019) 232–239, https://doi.org/10.1016/j.poly.2019.01.052.
[45] M. Amir, M. Aamir Qureshi, A. Khan, S.M. Nayeem, W. Ayoub Malik, S. Javed, Exploring the interaction of tepotinib with calf thymus DNA using molecular dynamics simulation and multispectroscopic techniques, Spectrochim. Acta A Mol. Biomol. Spectrosc. 308 (2024) 123678, https://doi.org/10.1016/j.saa.2023.123678.
[46] D.K. Jangir, S. Charak, R. Mehrotra, S. Kundu, FTIR and circular dichroism spectroscopic study of interaction of 5-fluorouracil with DNA, J. Photochem. Photobiol. B 105 (2011) 143–148, https://doi.org/10.1016/j.jphotobiol.2011.08.003.
[47] N. Shahabadi, M. Falsafi, M. Maghsudi, DNA-binding study of anticancer drug cytarabine by spectroscopic and molecular docking techniques, Nucleosides Nucleotides Nucleic Acids 36 (2017) 49–65, https://doi.org/10.1080/15257770.2016.1218021.
[48] N. Shahabadi, L. Heidari, Synthesis, characterization and multi-spectroscopic DNA interaction studies of a new platinum complex containing the drug metformin, Spectrochim. Acta A Mol. Biomol. Spectrosc. 128 (2014) 377–385, https://doi.org/10.1016/j.saa.2014.02.167.
[49] B. Nordén, F. Tjerneld, Structure of methylene blue–DNA complexes studied by linear and circular dichroism spectroscopy, Biopolymers 21 (1982) 1713–1734, https://doi.org/10.1002/bip.360210904.
[50] M.A. Husain, H.M. Ishqi, T. Sarwar, S.U. Rehman, M. Tabish, Interaction of indomethacin with calf thymus DNA: a multi-spectroscopic, thermodynamic and molecular modelling approach, Medchemcomm 8 (2017) 1283–1296, https://doi.org/10.1039/C7MD00094D.
[51] J. Saraswat, U. Riaz, R. Patel, In-silico study for the screening and preparation of ionic liquid-AVDs conjugate to combat COVID-19 surge, J. Mol. Liq. 359 (2022) 119277, https://doi.org/10.1016/j.molliq.2022.119277.